Chapter II

HYDROGEL NETWORKS FROM END-LINKED ELASTIN-LIKE ARTIFICIAL PROTEINS

1. Abstract

Recombinant proteins can be used to prepare artificial extracellular matrices for tissue engineering and other biomedical applications. Using genetic engineering methods, a telechelic protein bearing terminal thiols was designed from elastin- and fibronectin-derived repeating units and expressed in *Escherichia coli*. The recombinant protein, denoted ERE, was purified by inverse thermal cycling and obtained in good yield (100 mg per L of culture) with a free thiol content of approximately 90%. ERE was end-linked with tetrakis-vinyl sulfone-functionalized 4-arm star PEG to form hydrogel networks. The effects of varying the precursor concentration and cross-linker stoichiometry on the swelling ratio and mechanical properties of the hydrogels were studied in detail. The capacity for ERE hydrogels to serve as an artificial extracellular matrix was assessed by the encapsulation of mouse fibroblasts, which can survive the cross-linking reaction and exhibit a spread morphology within the gel.

2. Introduction

Hydrogels are cross-linked polymer networks that absorb a large amount of water. Due to their tissue-like elasticity and high water content, they have attracted significant attention as biomaterials that recapitulate essential features of cellular microenvironments for both tissue regeneration and fundamental biological studies. Hydrogels have been prepared from biomacromolecules such as proteins and polysaccharides, as well as from synthetic polymers such as poly(ethylene glycol) (PEG), poly(hydroxyethylmethacrylate) (pHEMA), and poly(lactic-*co*-glycolic) acid (PLGA) [1]. While biomacromolecular gels derived from natural proteins such collagen and fibrinogen can promote cell adhesion and are subject to proteolytic degradation, there are limited opportunities to engineer their physical and chemical properties. In contrast, synthetic polymers lack the instructive biological cues present in biomacromolecules but are versatile with respect to their molecular weight, topology, and chemical composition. Recombinant artificial proteins combine many of the advantages of naturally-derived biomacromolecules and synthetic polymers. A unique feature of recombinant proteins is the capacity to genetically encode and biologically synthesize a polypeptide chain with a precisely controlled sequence and molecular weight, and more importantly, with folded structures that specify function. An important example of recombinant artificial proteins for biomaterials applications are the artificial extracellular matrix (aECM) proteins [2]. These proteins combine structural elastin-like polypeptide (ELP) domains with cell-instructive amino acid sequences that promote cell adhesion or degradation by specific proteases. aECM proteins have been absorbed onto surfaces to promote cell-adhesion, cross-linked in films and hydrogels, and electrospun into fibers.

Hydrogel networks can be cross-linked by covalent bonds between artificial protein chains. The ε-amine of lysine is by far the most common target for cross-linking reagents, which include

bi- and trifunctional succinimidyl esters [3-5], hydroxymethyl phosphines [6-8], glutaraldehyde [9], diisocyanates [10], and others. However, as artificial protein designs become more complex in order to encode more advanced functionalities, the use of these established cross-linking chemistries may become limited by off target effects. For example, artificial proteins have been designed with enzymatic activity and well-folded three-dimensional structures that might be compromised or inactivated by lysine-specific cross-linkers, requiring either redesign of the protein sequence to remove Lys [11] or alternative cross-linking strategies. The same concerns are also relevant for the encapsulation of cells and biomolecules within hydrogels. Several approaches have been devised to overcome these issues including enzyme-mediated cross-linking [12, 13], bioorthogonal cross-linking reactions such as the strain-promoted azide-alkyne cycloaddition [14, 15], and genetically encoded SpyTag-SpyCatcher chemistry [16]. Still, these methods are somewhat limited by the efficiency of the cross-linking reactions or the ease with which they can be implemented.

Cysteine is perhaps the most promising of the 20 canonical amino acids for performing cross-linking of artificial proteins in the presence of cells or biomolecules, or for cross-linking artificial proteins with more complex structures and functions that could be affected by off-target effects. Cysteine occurs in proteins at an estimated frequency of 1.9% [17]. In contrast, lysine, which has been used extensively to modify and cross-link artificial proteins, occurs at a frequency of 5.9% [17]. Furthermore, cysteine often forms disulfide bonds in native proteins, which would render the thiol side chains of encapsulated cells or protein cargo inaccessible and inert to the cross-linking reaction. This is especially true in the extracellular space, which is regarded as an oxidizing environment.

The thiol side chain of cysteine is readily modified by molecules containing an activated alkene such as vinyl sulfones or maleimides to form stable thioether linkages. These reactions occur near physiological temperature and pH, making them broadly useful for bioconjugation and for applications in biomaterials. The latter has been demonstrated by Hubbell and coworkers, who have described two different examples of PEG-*co*-peptide hydrogels formed by cross-linking reactions between cysteine and vinyl sulfone. In the first example, short oligopeptides with terminal cysteine residues were reacted with 4-arm poly(ethylene glycol) vinyl sulfone to form a step growth network [18]. More recently, this approach has also been demonstrated with 4-arm PEG maleimide and 4-arm PEG acrylate [19]. In the second example, Hubbell and coworkers designed recombinant artificial proteins with sequences derived from fibrinogen and collagen [20]. The proteins contained 3-5 cysteines per chain and were cross-linked into hydrogel networks with PEG-divinyl sulfone. A similar approach was used by Kiick and coworkers to cross-link resilin-like artificial proteins with 4-arm PEG vinyl sulfone [21]. To date, the only example of ELP cross-linking through cysteines was described by Craig and coworkers, who designed an artificial protein containing repeats of the pentapeptide VPGCG and formed disulfide cross-links between the cysteine guest residues by oxidation with hydrogen peroxide [22].

This chapter describes the design and synthesis of a telechelic artificial protein ERE. Recombinant expression and non-chromatographic purification resulted in high yields of ERE with terminal cysteine residues in the reduced state. Hydrogel networks were formed by end-linking ERE with 4-arm PEG vinyl sulfone. The modulus and swelling behavior of ERE hydrogels could be tuned by varying the polymer concentration and functional group stoichiometry during cross-linking. Preliminary experiments indicate that ERE hydrogels can be formed in the presence of

fibroblast cells, enabling their encapsulation for three-dimensional cell culture and tissue engineering.

3. Materials and Methods

3.1 Plasmid Construction

The gene encoding the ERE protein was synthesized (Genscript, Piscataway, NJ) and subcloned into the pQE-80L expression vector (Qiagen, Valencia, CA) using the DH10B *Escherichia coli* cloning strain. The synthesized gene did not contain the 24 bp fragment encoding the MMP-1 degradable octapeptide near the C-terminus. In order to introduce this small fragment, complimentary oligonucleotide strands containing this sequence were synthesized (IDT, Coralville, IA), annealed by heating to 95 °C for five minutes followed by slow cooling, and phosphorylated with T4 polynucleotide kinase (New England Biolabs, Ipswich, MA). The annealed oligo strands contained overhangs that were used to direct ligation into the pQE-80L ERE plasmid that had been digested with *XhoI* (NEB). The resulting plasmid was used to transform the *Escherichia coli* expression strain BL21. The ERE gene sequence and amino sequence are given in Appendix A.

3.2 Protein Expression and Purification

Expression of the ERE protein was carried out in 1 L cultures in 2.8 L Fernbach flasks. A single colony of BL21/pQE-80L ERE was used to inoculate 5 mL of Luria broth (LB) supplemented with 100 μg mL^{-1} of ampicillin (BioPioneer, San Diego, CA). This culture was grown at 37 °C for 8 hr and then used to inoculate 25 mL of 2xYT containing 100 μg mL^{-1} of

ampicillin at a dilution of 1:100. This culture was grown overnight (approximately 12 hr) at 37 °C and then used to inoculate 1 L of Terrific broth containing 100 μg mL^{-1} of ampicillin at a dilution of 1:50. The culture was grown at 37 °C until the optical density at 600 nm (OD_{600}) reached approximately 0.9-1, at which point protein expression was induced by the addition of 1 mM isopropyl β-D-1-thiogalactopyranoside (IPTG) (BioPioneer). Expression proceeded for 5 hr and the cells were harvested by centrifugation at 6000 *g*, 4 °C for 8 min. The cell pellets (approximately 9 g per L of culture) were resuspended in 25 mL of TEN buffer (10 mM Tris, 1 mM EDTA, 100 mM NaCl) supplemented with 5% (v/v) glycerol, 0.1% (w/v) sodium deoxycholate (Sigma), 0.1% (v/v) TritonX-100 (Sigma) and frozen at -20 °C.

The cell resuspension was thawed and treated with 10 μg mL^{-1} DNase I (Sigma, St. Louis, MO), 10 μg mL^{-1} RNase A (Sigma), 1 mM pheynlmethylsulfonyl fluoride (Gold Biotechnology, Olivette, MO), and 5 mM $MgCl_2$ at 37 ^oC for 30 min with agitation. The cells were lysed by sonication with a probe sonicator (QSonica, Newton, CT), and 1% (v/v) β-mercaptoethanol (β-ME) (Sigma) was added to the lysate to reduce disulfide bonds for 1 hr on ice. Purification of the ERE protein from the *E. coli* lysate was accomplished by inverse temperature cycling [23]. The lysate was centrifuged at 39,000 *g*, 4 °C for 1 hr to remove insoluble cell debris. Crystalline NaCl was added to the supernatant to a final concentration of 2 M, and the solution was agitated at 37 °C for 1 hr. The coacervate phase containing ERE was collected by centrifugation at 39,000 *g*, 37 °C for 1 hr. ERE was extracted from the resulting pellet with TEN buffer containing 1% (v/v) β-ME overnight at 4 °C. This procedure was repeated twice with 30 min centrifugation steps. After the third and final cycle, the pelleted protein was resuspended in TEN buffer containing 5 mM tris(hydroxypropyl)phosphine (THP) (Santa Cruz Biotechnology, Dallas, TX) rather than β-ME. After reduction for 2 hr at 4 °C, the buffer and THP were removed by desalting using Zeba 7 kDa

MWCO columns equilibrated with degassed water (LCMS grade, Sigma). The eluted ERE protein was frozen immediately, lyophilized for 72 hr, and stored at -80 °C under argon. Typical yields were 100 mg of lyophilized ERE per L of culture.

The ERE protein could also be obtained from 10 L cultures in a BioFlo 3000 fermentor (New Brunswick, Edison, NJ). Typical yields from fermentation were greater than 300 mg per L. However, due to the limited throughput of the desalting step and concerns about eventual oxidation of the cysteine residues in ERE during storage, smaller batches of proteins were preferred.

3.3 Protein Characterization

The purity and molecular weight of ERE were assessed by sodium dodecyl sulfate polyacrylamide gel electrophoresis (SDS-PAGE), Western blotting, and intact liquid chromatography-mass spectrometry (LCMS) with electrospray ionization (ESI). For SDS-PAGE, lyophilized ERE was dissolved at 5 mg mL^{-1} in 100 mM sodium phosphate, 1 mM EDTA, pH 8. This solution was diluted 1:10 into SDS loading buffer, and 5 μL was loaded on a 10-well NuPage Novex 4-12% Bis-Tris gel (Thermo Fisher Scientific, Waltham, MA). Protein electrophoresis was performed in MES-SDS running buffer (Boston BioProducts, Ashland, MA) at 180 V for 45 min. The proteins were visualized with InstantBlue protein stain (Expedion, San Diego, CA).

The fraction of free cysteines in the purified ERE protein was measured by Ellman's assay. Lyophilized ERE protein was dissolved in reaction buffer (100 mM sodium phosphate, 1 mM EDTA, pH 8) at a concentration of 5 mg mL^{-1}. A stock solution of Ellman's reagent, (5,5'-dithio-bis-[2-nitrobenzoic acid]), (Sigma) was also prepared at 5 mg mL^{-1}. In a cuvette, 250 μL of protein solution and 50 μL of Ellman's stock solution were added to 2.5 mL of reaction buffer. The reaction was incubated at ambient temperature for 15 min and the absorbance at 412 nm was

measured on a Cary 50 spectrophotometer. The extinction coefficient of the reaction product, 2-nitro-5-thiobenzoate (14,150 M^{-1} cm^{-1}) [24], was used to determine the concentration of free thiols.

3.4 Hydrogel Cross-linking

Cross-linking with PEG-4VS was performed under denaturing conditions in 0.1 M sodium phosphate, 6 M guanidinium chloride, 0.4 M triethanolamine (TEOA) (Sigma) at pH 7.4. To prepare 15 wt% gels (initial concentration of total polymer), lyophilzed ERE protein (150 mg) was dissolved in 1 mL of degassed cross-linking buffer. PEG-4VS (Jenkem USA, Plano, TX) was dissolved at the same concentration in degassed 0.4 M TEOA, pH 7.4. The solutions were sonicated for 2 min in an ultrasonic bath and centrifuged for 1 min, 10,000 *g* to remove air bubbles. In a microcentrifuge tube, 271 μL of the cross-linker solution was added to 1 mL of the protein solution. This volumetric ratio gives a nominal 1:1 stoichiometric ratio of vinyl sulfone to thiol functional groups. The actual stoichiometric ratio will vary slightly based on fraction of free thiols in the ERE protein preparation and the functionalization of the PEG-4VS. The mixture was vortexed and droplets (50-70 μL) were pipetted onto glass slides that had been treated with SigmaCote (Sigma) according to the manufacturer's protocol. A second treated glass slide was placed on top, separated by a spacer cut from a sheet of silicone rubber (McMaster-Carr, Santa Fe Springs, CA) (1 mm or 2 mm). The slides were clamped together with binder clamps. The cross-linking reaction was allowed to proceed overnight (>12 hr). Gels were also prepared in this manner with different initial polymer concentrations (7.5, 10, 15, 20, 25 wt%) at a constant 1:1 vinyl sulfone to thiol stoichiometry, and with different functional group stoichiometry (0.6:1, 0.8:1, 1:1, 1.2:1, 1.4:1 vinyl sulfone to thiol) at a constant polymer concentration of 15 wt%.

A second cross-linking protocol that omitted the guanidinium chloride and triethanolamine was also assessed. ERE and PEG-4VS were dissolved at 5, 7.5, and 10 wt% in HEPES buffered saline (25 mM HEPES, 150 mM NaCl, pH 7.4) without triethanolamine. Solutions of ERE and PEG-4VS at equal concentration were mixed at a 1:1 vinyl sulfone to thiol stoichiometry in a microcentrifuge tube, vortexed, and pipetted onto a treated glass slide with 1 mm spacers as described. The gels were cured overnight.

3.5 Equilibrium Swelling and Sol Fraction Determination

Hydrogel disks (50 μL in the as-prepared or unswollen state) were swollen for 48 hours in 1 mL of sterile distilled, deionized (ddH_2O). The amount of unreacted material removed from the gel was estimated by measuring the protein concentration using a bicinchoninic acid assay (BCA, Pierce, Rockford, IL) according to the manufacturer's protocol. A standard curve was generated using ERE solutions of known concentration prepared from lyophilized protein. After removing the ddH_2O, the gels were swollen in phosphate buffered saline (PBS) (1.5 mM KH_2PO_4, 4.3 mM Na_2HPO_4, 137 mM NaCl, 2.7 mM KCl, pH 7.4) for 48 hr and the swollen mass was determined by weighing the gels on an analytical balance (Mettler Toledo, Columbus, OH). The gels were transferred to ddH_2O, which was changed five times over the course of 3 days to remove the salts. The gels were frozen in microcentrifuge tubes and lyophilized so that the dry mass could be measured. The equilibrium swelling ratio, Q_m, was determined by dividing the swollen mass by the dry mass. Six replicates were performed for each gel.

3.6 Rheological Characterization

Rheological measurements were performed on a TA Instruments (New Castle, DE) ARES-RFS strain-controlled rheometer with a parallel-plate geometry (8 mm diameter). Hydrogel disks were cut to this size from larger samples using an 8 mm diameter biopsy punch (Miltex, York, PA) and loaded between the sample plates according to the protocol described by Meyvis *et al* [25]. Briefly, the gap between the upper and lower plates was lowered until a normal force was detected. The storage modulus (*G'*) was then measured at 1% strain amplitude, 5 rad s^{-1}, 25 °C. The gap was then lowered by 20 μm and the measurement of *G'* was repeated. This process was continued until *G'* at 5 rad s^{-1}, 1% strain amplitude reached a constant value. A strain sweep test from 0.1-10% was performed to confirm the linear viscoelastic regime of each sample at 10 rad s^{-1} and 25°C. Following the strain sweep, a frequency sweep was performed at 5% strain amplitude, 25 °C over an angular frequency range of 100 to 0.1 rad s^{-1}. Three replicates were performed for each gel.

3.7 Dynamic Oscillatory Time Sweep

The gelation time was determined by performing a dynamic oscillatory time sweep experiment on the ARES-RFS equipped with a 25 mm parallel plate geometry and Peltier temperature controller set to 37 °C. Solutions of ERE and PEG-4VS were prepared in HEPES buffered saline at 5, 7.5, and 10 wt%, vortexed to mix, and centrifuged briefly to remove bubbles. In a microcentrifuge tube, 54.2 μL of PEG-4VS solution was added to 200 μL of ERE solution giving a 1:1 vinyl sulfone to thiol stoichiometry. The mixture was vortexed briefly before pipetting 200 μL onto the lower plate of the rheometer. The gap height was adjusted incrementally to 200 μm and the edge of the gel was covered with paraffin oil. This process had a typical lag time of approximately 2 minutes from the time at which the two components were mixed until data

collection began. A time sweep experiment was performed at 5% strain amplitude, 10 rad s^{-1}. The gelation time is taken as the time at which *G'* and *G"* intersect. Three replicates were performed for each concentration.

3.8 Encapsulation of Fibroblasts

NIH 3T3 mouse fibroblasts (American Type Culture Collection, Manassas, VA) were maintained at 37 °C with 5% CO_2 in Dulbecco's Modified Eagle Medium (DMEM) (Life Technologies, Carlsbad, CA) with 10% (v/v) bovine serum (Life Technologies), and 1% (v/v) penicillin/streptomycin (Life Technologies). At ≈80% confluence, cells were detached with 2 mL of trypsin (0.05%) – EDTA (0.02%) solution (Life Technologies) for 5 min at ambient temperature followed by addition of 8 mL of complete growth medium to neutralize the trypsin. The cell suspension was centrifuged at 200 *g* for 3 minutes. After removal of the medium, the pelleted cells were washed in 10 mL of HEPES buffered saline (HBS), and centrifuged again. Finally, the cells were resuspended in 1 mL HBS and counted using a hemocytometer.

Cells were encapsulated in 5, 7.5, and 10 wt% ERE hydrogels cross-linked at a 1:1 vinyl sulfone to thiol stoichiometry. ERE and PEG-4VS were dissolved at these concentrations in HBS, pH 7.4 and sterile-filtered using a 0.2 μm centrifugal filter (Corning, Corning, NY). Cells were aliquoted in microcentrifuge tubes and centrifuged to remove the buffer. The pellet was resuspended in the ERE solution at a concentration of 3 x 10^6 cells mL^{-1} and mixed with the PEG-4VS solution by gentle vortexing. A 30 μL droplet was pipetted onto a 35 mm glass bottom dish (MatTek, Ashland, MA). The gelation mixtures were cured at 37 °C in a humidified incubator. Based on the results of the gelation kinetics experiments, 10 wt% gels were cured for 1 hr prior to adding 3 mL DMEM (without phenol red) + 10% bovine serum + 1% penicillin/streptomycin; 7.5

wt% gels were cured for 1.5 hr, and 5 wt% gels were cured for 2 hr. Following the addition of media, the gels were incubated at 37 °C with 5% CO_2. The medium was changed the next day.

The viability of fibroblasts encapsulated in hydrogels was determined using a Live/Dead stain (Invitrogen, Carlsbad, CA) 3 days post-encapsulation. Briefly, after removal of DMEM, the hydrogel was washed with 3 mL of PBS. The Live/Dead staining solution (2.5 mL), which contained 4 μM ethidium homodimer-1 (EthD-1) and 2 μM calcein AM in PBS, was added to the cell-laden hydrogel and incubated for 45 minutes at room temperature. Following incubation, the staining solution was removed and the hydrogels were washed with PBS (3 mL) and covered in cell culture medium (3 mL). Laser scanning confocal microscopy (LSM 510, Zeiss, Irvine, CA) was used to visualize the stained cells. A 20x/0.3 long working distance objective was used for all images. The calcein fluorophore was detected by excitation at 488 nm with an argon laser and a 505 nm LP emission filter. The EthD-1 fluorophore was detected by excitation at 543 nm with a He/Ne laser and a 630 nm LP emission filter. Images were acquired as z-stack sections every 10 μm over a 200 μm thick region of the gel beginning at least 100 μm away from the coverslip. The images were analyzed with ImageJ (NIH, Bethesda, MD) to generate max intensity projections in the z-direction.

4. Results and Discussion

4.1 Protein Design and Synthesis

The multiblock, telechelic protein ERE (Figure II-1 a and b) was designed with an amino acid sequence that encodes the desired biological activity (cell-adhesion and proteolytic degradation) and physical properties (cross-linking sites and elastin-like domains). ERE contains two domains that confer biological activity required for cell encapsulation. The first is a cell-

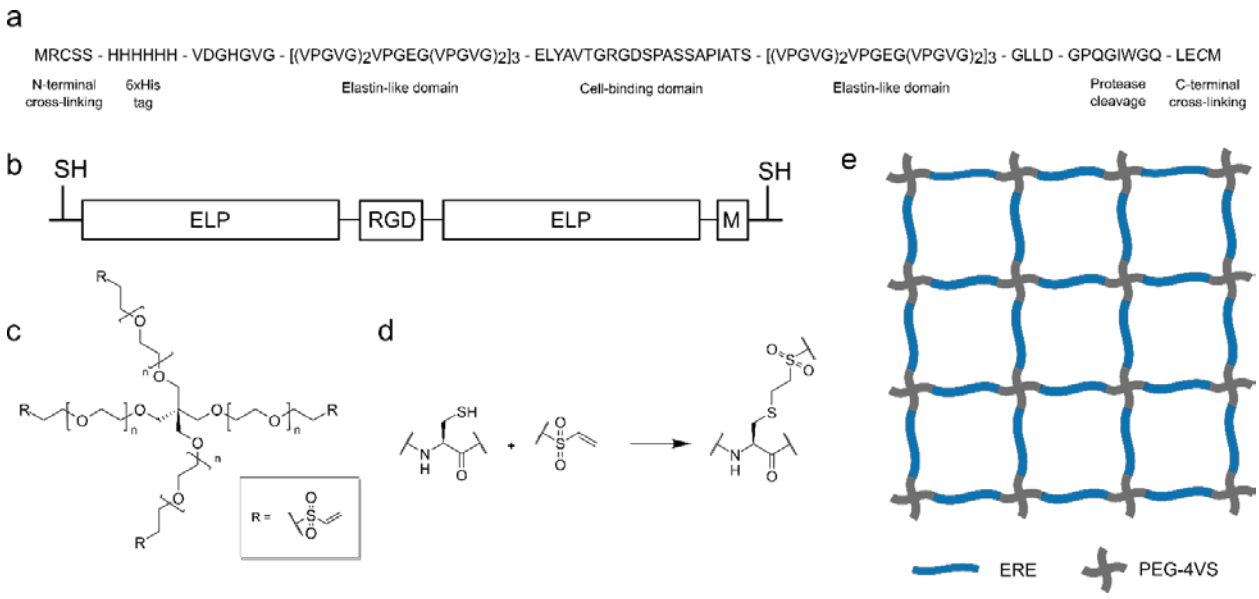

Figure II-1. Sequence of ERE and cross-linking scheme. (**a**) Amino acid sequence and (**b**) multiblock structure of ERE, which is composed of elastin-like polypeptide (ELP) endblocks, a cell-binding domain R, an MMP-1-degradable sequence M, and terminal cysteine residues. (**c**) 4-arm poly(ethylene glycol) tetrakis-vinyl sulfone (PEG-4VS) is used to end-link ERE through a Michael-type conjugate addition of the thiol side chain of cysteine to vinyl sulfone (**d**), resulting in a step-growth network idealized in (**e**).

binding domain, denoted R, that promotes cell adhesion through integrin receptors. The R domain consists of 17 amino acids from a solvent exposed loop in the tenth type III repeat of human fibronectin [26, 27]. This loop contains the RGD (Arg-Gly-Asp) tripeptide that has been widely used in biomaterials prepared from artificial proteins and from synthetic peptides [28]. The second biologically active domain encoded in the ERE protein is the octapeptide sequence GPQGIWGQ that can be digested by several matrix metalloproteinases (MMPs). This peptide sequence is based on degradable sequences in various collagen proteins and was originally designed as one of many substrates to study the sequence specificity of MMPs [29]. It was found to be a good substrate for several MMPs including collagenases (MMP-1 and MMP-8), gelatinases (MMP-2 and MMP-9),

stromelysin (MMP-3), and matrilysin (MMP-7). Several biomaterial designs have incorporated this peptide or similar sequences to create degradable scaffolds that allow encapsulated cells to remodel their local environment in order to spread or migrate [18, 30]. Including this sequence between the cross-linking sites in ERE is expected have a similar effect in this work.

ERE contains unique cysteine residues at the N- and C-termini for end-linking with thiol-reactive cross-linkers. The remainder of the protein is composed primarily of elastin-like repeats (E), meaning that these domains are likely to determine the physical properties of hydrogels prepared from ERE. ELPs have received signification attention as biomaterials for tissue engineering and are well known for their lower critical solution temperature (LCST) transition. At temperatures below their LCST, ELPs are soluble and unstructured. At temperatures above their LCST, ELPs aggregate into a protein-rich coacervate phase. Inverse thermal cycling at temperatures above and below the LCST can be used to separate ELPs from proteins and other contaminants that do not possess this transition behavior as a low-cost alternative to chromatographic purification [23]. However, in many cases, the phase transition of ELPs in biomaterials also results in protein aggregation and heterogeneous network structures at physiological temperature [3, 31]. This can alter the mechanical properties of the material and results in poor optical transparency, obstructing the observation of encapsulated cells by light microscopy. Mixing hydrophilic poly(ethylene glycol) with ELPs that have a low LCST has been reported to improve the transparency, but the effect is limited [31]. To address this problem, the elastin-like domains in ERE are more hydrophilic sequences with guest residues occupied by valine and glutamic acid at a ratio of 4:1. The LCST of an ELP with this composition was reported to be approximately 75 °C at a neutral pH and an ionic strength of 150 mM [32], which are typical physiological conditions. By increasing the ionic strength of the ELP solution, the LCST can be

suppressed significantly. In this way, it was anticipated that the ERE protein could be purified by the inverse thermal cycling method yet remain transparent when cross-linked into a hydrogel and swollen at physiological temperature (37 °C), pH, and salt concentration.

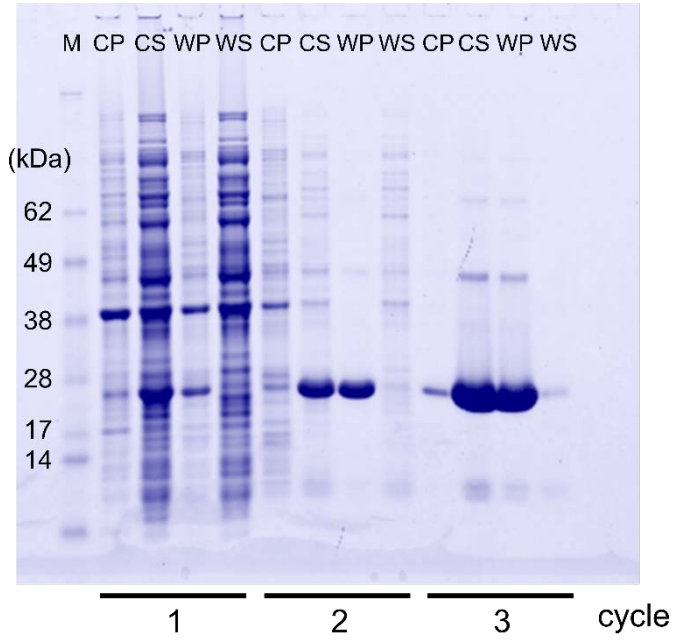

Figure II-2. Temperature cycling purification of ERE. ERE was purified from the *E. coli* lysate by three rounds of temperature cycling above and below the lower critical solution temperature. The target protein is soluble in the cold step (4 °C, 100 mM NaCl) and aggregates into a protein-rich coacervate phase in the warm step (37 °C, 2 M NaCl). The apparent molecular weight of ERE (approx. 25 kDa) is slightly greater than the calculated molecular weight (18.5 kDa), but this is common for elastin-like proteins. The expected molecular weight was confirmed by ESI-MS.

The ERE protein was produced in *Escherichia coli* strain BL21 and purified by three rounds inverse temperature cycling above and below the LCST of the protein. Thermal cycling with hydrophilic ELP sequences has rarely been reported. However, ERE is expressed at high levels in

E. coli and increasing the ionic strength of the lysate by addition of 2 M NaCl was found to be sufficient to shift the LCST to below 37 °C. Raising the temperature above 37 °C and agitating the solution caused the formation of ERE aggregates that could be separated by centrifugation. The ERE proteins were extracted from the pelleted fraction by resuspension in a low ionic strength (100 mM NaCl) buffer at 4 °C. To prevent thiol oxidation, β-mercaptoethanol (βME) was included in the solution throughout the purification. After three cycles, ERE was successfully purified from the *E. coli* lysate proteins (Figure II-2). Tris(hydroxypropyl) phosphine was used to reduce protein disulfides and β-ME/cysteine adducts. The buffer, salts, and reducing agents were removed by gel filtration chromatography and the final product was obtained by lyophilization. The typical yields for ERE were 100 mg per L of culture. The molecular weight of the purified protein was confirmed by intact LC-MS with electrospray ionization ($M_{\text{calcd.}}$ = 18476, $M_{\text{obs.}}$ = 18477).

4.2 Evaluation of Protein Free Thiol Content

The free thiol content of purified ERE was evaluated with Ellman's assay, in which cysteine reacts with (5,5'-dithio-bis-[2-nitrobenzoic acid]) (DTNB) to produce a yellow color corresponding to the 2-nitro-5-thiobenzoate ion (TNB^{2-}) [33]. The absorbance at 412 nm was used to calculate the concentration of TNB^{2-}, which is equal to the concentration of free thiols. For a solution of lyophilized ERE dissolved at 5 mg mL^{-1}, the concentration of free thiols measured by Ellman's assay was found to be 88% of the expected amount based on the protein concentration and the assumption that each ERE protein contains two cysteines (Table II-1). The discrepancy between the observed thiol concentration and the expected thiol concentration is likely due to the formation of higher order protein oligomers linked by intermolecular disulfides, cyclization of ERE by an intramolecular disulfide bond, or other impurities with unknown cysteine contents. To

confirm that the TNB^{2-} detected in Ellman's assay was not due to residual reducing agents (e.g. THP or β-ME) in the ERE preparation that could potentially cleave the disulfide bond in DTNB, the ERE protein solution was filtered through a 10 kDa MWCO column. The column is expected to retain ERE (18.5 kg mol^{-1}) but allow the passage of small molecules such as THP (209 g mol^{-1}) and β-ME (78 g mol^{-1}) into the filtrate. When the filtrate was analyzed by Ellman's assay, the absorbance at 412 nm was too low to be accurately measured (data not shown), confirming that the observed thiol concentration reported in Table II-1 is due to free cysteines on the ERE protein.

Measured [thiol] (μM)	**[ERE] (μM)**	**mol free thiol/ mol protein**
42.6 ± 1.4	24.1	1.76 ± 0.06

Table II-1. Concentraion of free thiols determined by Ellman's assay. The thiol concentration determined from the absorbance of NTB^{2-} was divided by the concetration of protein in the reaction mixture to obtain an estimate of the number of free thiols per protein chain.

The purified ERE protein was also characterized by non-reducing SDS PAGE to determine its oligomerization state (Figure II-3 and Table II-2). Intermolecular disulfide bonds between cysteines on different ERE protein chains lead to chain extension into higher order protein oligomers while intramolecular disulfide formation between the N- and C-terminal cysteines of one protein chain (or an extended chain) leads to cyclization. Samples of ERE were prepared in SDS loading buffer with and without 5% (v/v) β-ME as a disulfide reducing agent. The sample containing β-ME was also boiled for 3 min to improve the reduction. Visualization of the proteins

by Coomassie staining (Figure II-3 a) or Western blotting (Figure II-3 b) after electrophoresis revealed a strong band near the expected molecular weight in both samples. Much weaker bands were also observed in the Coomassie-stained gel at the molecular weight corresponding to an ERE dimer, but higher order oligomers were not observed. The monomeric ERE bands contain a small shoulder at lower apparent molecular weights that is attributed to the cyclized monomer. (The linear and cyclic monomers are not well resolved for the ERE protein, but are for other telechelic proteins that will be considered in next chapters.)

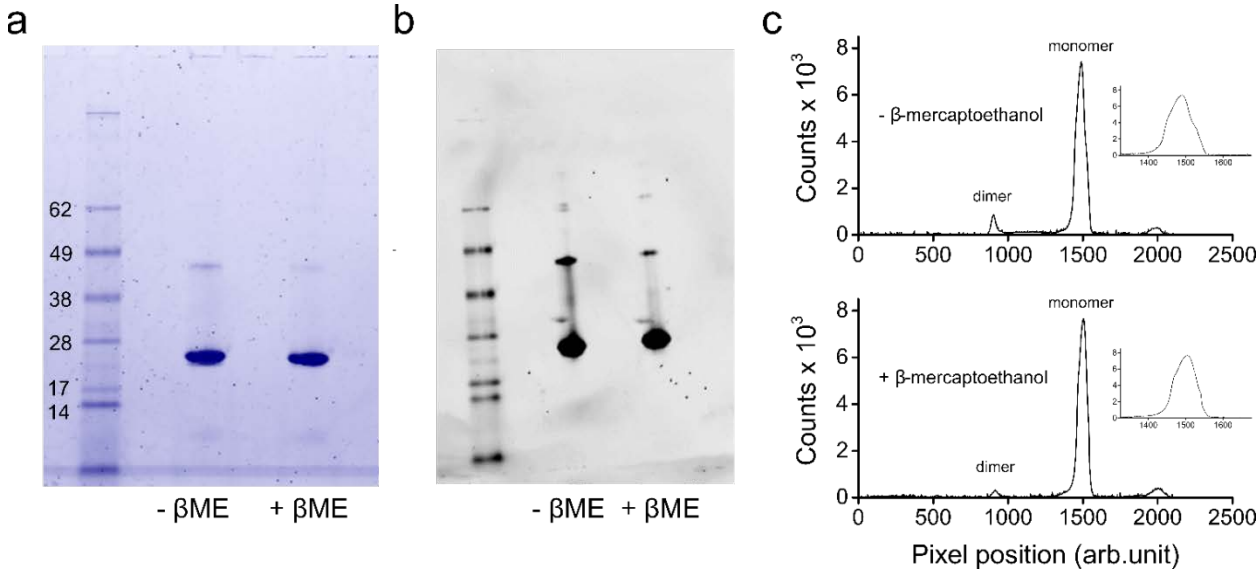

Figure II-3. Assesment of protein purity and oligomerization state by non-reducing SDS-PAGE. (**a**) Purified ERE protein is primarily monomeric by SDS-PAGE in samples prepared with or without β-mercaptoethanol as disulfide reductant, confirming that the protein thiols are reduced following purification. (**b**) The presence of the 6xHis tag at the N-terminus was confirmed by Western blotting using an penta-his antibody. (**c**) The lane profiles of the gel in (a) were quantified by gel densitometry to determine the fraction of monomer, dimer, and higher order species in the ERE preparation.

The average pixel intensity along each lane is plotted in Figure II-3 c. The peak corresponding the dimer is only slightly greater for the ERE sample prepared without β-ME than for the ERE sample prepared with β-ME. Integration of the ERE peaks as well as a small impurity at approximately 10 kDa was used to estimate the free thiol content by assuming that dimers contain one free thiol per protein, linear monomers contain two free thiols per protein, and that cyclic monomers do not contain any free thiols (Table II-2). The unknown impurity accounts for only about 2% of the total peak area and is assumed to not contribute to the sample thiol content. For the ERE sample without β-ME, the estimated free thiol content from the observed distribution of monomers, dimers, and cyclized protein is in excellent agreement with the thiol content measured by Ellman's assay (Table II-1) (1.78 vs. 1.76). From these experiments, it is concluded that ERE can be synthesized in *E. coli* and purified from the lysate by inverse temperature cycling, and that the terminal cysteine residues are in the reduced state and should be available for covalent cross-linking.

SDS-PAGE band	**Fraction total area**	**Thiols per chain**	**mol free thiol/ mol protein**
dimer	0.04	1	0.04
linear monomer	0.87	2	1.74
cyclic monomer	0.07	0	0
impurity (approx. 10 kDa)	0.02	unknown (assume 0)	0
Total	**1**	**-**	**1.78**

Table II-2. Quantiation of the oligomerization state of purified ERE protein by gel densitomtry. The area of the peaks assigned as the linear monomer, cyclic monomer, dimer, and impurity (at approximately 10 kDa) in Figure II-3 (c, *top*) were each divided by the total peak area to obtain the fraction of ERE protein in a particular oligomerization state (column 2). The fractions were multipled by the expected number of thiols per chain (column 3) to obtain an estimate for the number of free thiols per protein (column 4).

4.3 Hydrogel Formation and Characterization

The purified ERE protein was used to prepare hydrogel networks by end-linking with 4-arm PEG tetrakis-vinyl sulfone (PEG-4VS) (Figure II-1 c). The thiol side chains of the cysteine residues at the protein termini react with the vinyl sulfone functional groups at each end of the star PEG through a Michael-type conjugate addition to form a thioether bond (Figure II-1 d). An idealized step-growth network resulting from this reaction is shown in Figure II-1 e. Hydrogels formed upon mixing a solution of ERE protein and a solution of PEG-4VS. In this work, the two macromer solutions were always prepared at equal concentration and mixed at a volumetric ratio that gave the desired functional group stoichiometry (*r*). The ERE solution was prepared by dissolving lyophilized protein in 0.1 M phosphate buffer containing 0.4 M triethanolamine, an organic base that promotes the addition of the thiol nucleophile to the electrophilic alkene, and 6 M guanidinium chloride, a protein denaturant. Guanidinium chloride (GndCl) is not required for cross-linking ERE proteins but is used in subsequent chapters to disrupt the association between artificial proteins containing domains that form intermolecular coiled coils. The cross-linker solution was prepared by dissolving PEG-4VS in 0.4 M triethanolamine. After mixing the protein and cross-linker solutions, the gelation mixture was cured between glass slides separated by rubber spacers. Hydrogel disks formed in this way could be removed from the glass surface and characterized in the as-prepared or unswollen state, or could be swollen in buffer to remove the denaturant as well as the unreacted protein and PEG-4VS.

The typical results of cross-linking 15 wt% ERE and PEG-4VS solutions at a 1:1 vinyl sulfone to thiol ratio are shown in Figure II-4. The gels are tan to light brown in the as-prepared state due the absorbance of the ERE protein (Figure II-4 a), and transparent when swollen in PBS (Figure II-4 b). The gels were characterized by small amplitude oscillatory shear rheology (SAOS)

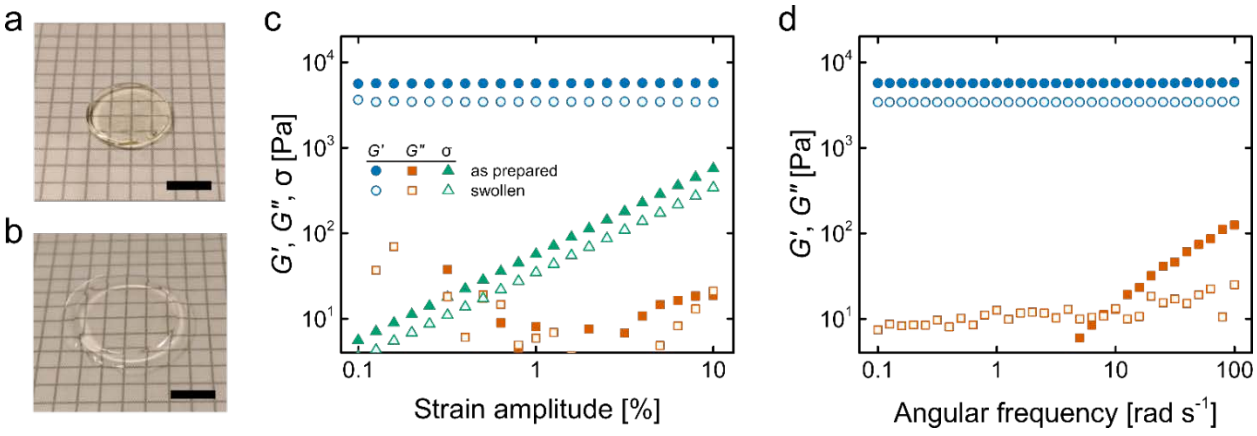

Figure II-4. ERE Hydrogels. Photographs of ERE hydrogels in the (**a**) as-prepared (unswollen) state and (**b**) swollen in PBS, pH 7.4. The gels were cross-linked at 15 wt% total polymer and 1:1 VS:SH stoichiometry. (**c**) Dynamic oscillatory rheology strain sweep of ERE hydrogels in the as-prepared (filled symbols) and swollen (open symbols) states at 10 rad s^{-1}, 25 °C. The storage modulus (*G'*, circles) is much greater than the loss modulus (*G"*, squares), which is difficult to measure accurately. The stress (σ, triangles) increases linearly with the stain amplitude. (**d**) Dynamic oscillatory rheology frequency sweep of ERE hydrogels at 5% strain amplitude, 25 °C. In both (c) and (d), *G'* in the as-prepared state is greater than the swollen state due to the decrease in the density of elastically effective chains upon swelling. The scale bars in (a) and (b) are 1 cm.

in both the as-prepared state and after swelling for 48 hr in phosphate buffered saline (PBS, pH 7.4). The strain sweeps (Figure II-4 c) of these materials demonstrate that the storage modulus (*G'*) is nearly constant over the entire range of strain amplitudes tested (0.1-10%), indicating that the material response is linear in this regime. The frequency sweeps of 15 wt% hydrogels (Figure II-4 d) in both the swollen and as-prepared states are characterized by *G'* that are nearly independent of the oscillation frequency. The storage moduli are also more than two orders of magnitude greater than the loss moduli (*G"*), indicating that the response of the hydrogel to deformation is primarily

elastic. As expected, the swollen gels are softer than the as-prepared gels because the chain density decreases as upon the absorption of additional solvent.

The initial polymer concentration in the cross-linking reaction and the stoichiometry (r) of the vinyl sulfone and thiol functional groups were varied systematically in order to determine their effects on the macroscopic properties of ERE networks: the storage modulus G' and the mass swelling ratio Q_m. Hydrogels were prepared from protein and PEG-4VS solutions at 7.5, 10, 15, 20, and 25 wt% while maintaining a vinyl sulfone to thiol stoichiometry of 1:1 (Figure II-5). In both the as-prepared and swollen states, the hydrogels became stiffer as the initial polymer concentration was increased. The mass swelling ratio Q_m, which is equal to the swollen hydrogel mass divided by the dry polymer mass, decreased as the initial polymer concentration was increased. In this way, the modulus of the ERE-VS hydrogels could be tuned over a range of 0.7 kPa to 12 kPa.

In the course of the experiments to determine the mass swelling ratio, the protein component of the sol fraction, or the fraction of ERE protein that was not connected to the network, was collected and quantified by the bicinchoninic acid (BCA) assay. Following a similar analysis of PEG-*co*-peptide hydrogels by Lutolf and Hubbell [18], the sol fraction was used to estimate the extent of reaction p between the thiol and vinyl sulfone groups as well as the concentration of elastically effective chains (ν) and the cross-link density (μ) by Miller-Macosko theory [34]. These data are summarized in Table II-3. The extent of reaction p increases from 0.78 for networks prepared at 7.5 wt% to 0.88 for networks prepared at 25 wt%, suggesting that a higher concentration of functional groups drives the reaction closer to full conversion. Similar results

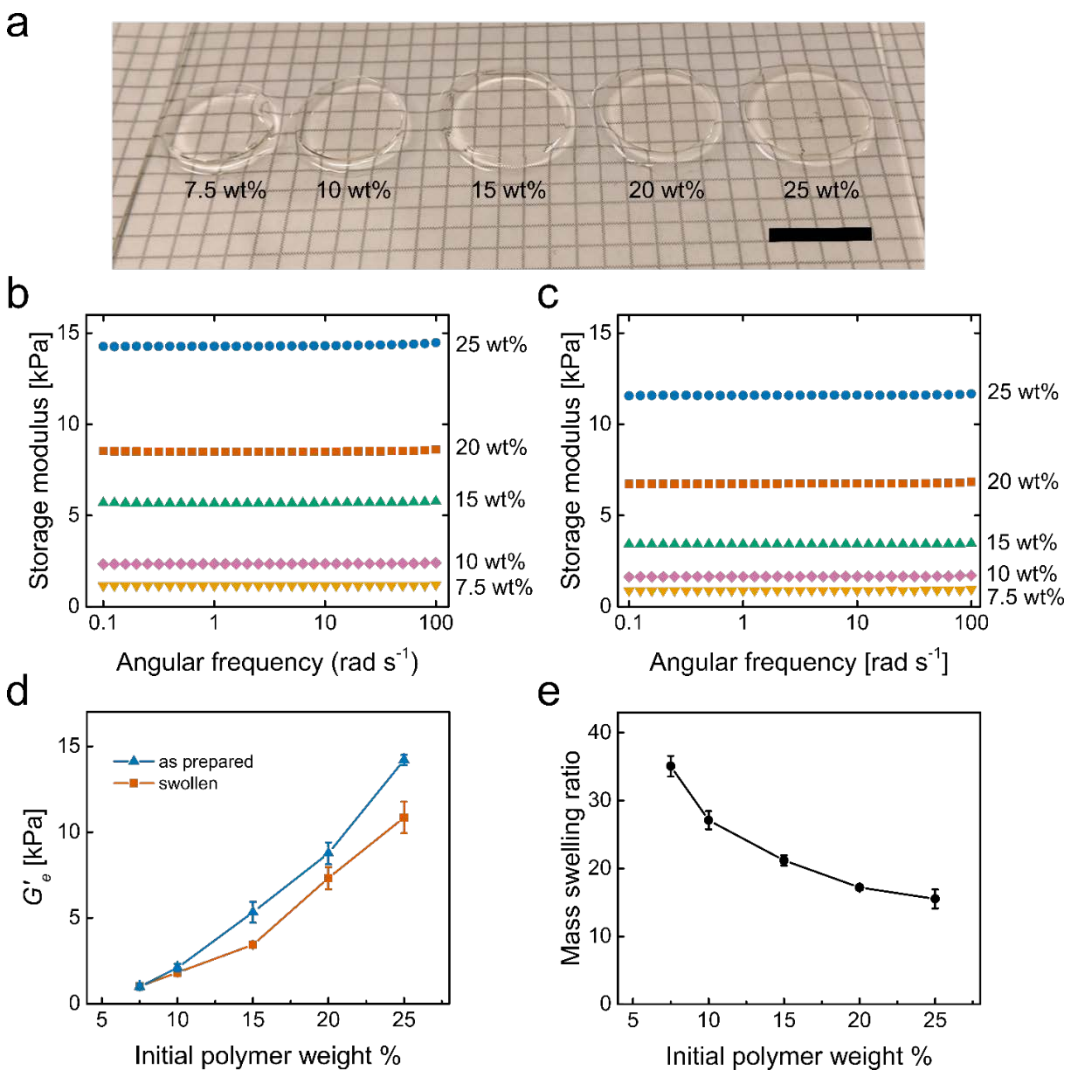

Figure II-5. Variation of the initial polymer concentration between 7.5-25 wt%. (**a**) Photographs of swollen ERE hydrogels. (**b**) Representative frequency sweep experiments show the storage moduli of ERE hydrogels at various initial polymer concentrations in the as-prepared state. (**c**) Representative frequency sweep experiments show the storage moduli of ERE hydrogels at various initial polymer concentrations after swelling to equilibrium in PBS. (**d**) For each initial concentration, the equilibrium modulus G'_e, which is defined here as G' at 1 rad s^{-1}, is plotted for the as-prepared and swollen gels (n = 3, avg. ± s.d.). (**e**) The mass swelling ratio after swelling to equilibrium in PBS decreases as the initial polymer concentration is increased (n = 6 gels, avg. ± s.d.). All frequency sweep experiments were performed at 5% strain amplitude, 25 °C. The scale bar in (a) is 1 cm.

were reported for the reaction of cysteine-containing peptides and PEG-4VS in ref. [18], with p varying from 0.80 for a 5 wt% gelation mixture to 0.88 for a 40 wt% gelation mixture.

The calculated values of ν and μ were then used to compute a theoretical shear modulus by two theories of rubber elasticity: the affine approximation and the phantom network approximation [35]. In the affine approximation, the cross-links are considered fixed in space with no thermal fluctuations. When a cross-linked network is stretched from its original length L_0 to a deformed length $L = \lambda L_0$, the end-to-end vector of a chain segement between cross-link points is assumed to undergo the same deformation. This leads to the following expression for the shear modulus (cross-linked in a θ-solvent):

$$G_{af} = \nu RT\left(\frac{\varphi}{\varphi_0}\right)^{1/3} \qquad \text{(Equation II-1)}$$

where R is the gas constant, T is the temperature, and φ and φ_0 are the polymer volume fractions in the swollen and as-prepared states. The polymer volume fractions were determined from the mass swelling ratio by assuming that the hydrogel density is equal to the density of water (≈ 1 g mL^{-1}) and the dry polymer density is equal the mass average of the density of elastin (1.3 g mL^{-1}) [36] and the density of 10,000 g mol^{-1} PEG (1.2 g mL^{-1}) [37]. The theoretical modulus can also be determined by the phantom network approximation, which allows for the fluctuation of the cross-link points in space. Because these fluctuations increase the entropy and lower the free energy per chain, the phantom network modulus is lower than the affine modulus. The expression for the modulus is:

$$G_{ph} = (\nu - \mu)RT\left(\frac{\varphi}{\varphi_0}\right)^{1/3} \qquad \text{(Equation II-2)}$$

The moduli of ERE gels computed from Eq. II-1 and Eq. II-2 for the as-prepared state ($\varphi = \varphi_0$) and swollen state are listed in Table II-4 along with the experimental values of the equilibrium modulus G'_e (plotted in Figure II-5 d). The experimental values of the modulus fall between the predicted affine and phantom network values, and are typically closer to the phantom network prediction. It should be noted that this analysis does not account for elastically ineffective chains due to loop formation, consumption of thiols by disulfide bond formation, or chain entanglements. The expressions for the moduli also assume ideal behavior of the chain segments between cross-links. Non-idealities are likely present in ERE gels to some extent, and will contribute to the swelling behavior and modulus in different ways. Intramolecular disulfide bonds generate looped ERE chains that cannot react with PEG-4VS and should therefore be part of the sol fraction. Intermolecular disulfide bonds generate extended ERE chains with increased molecular weight between cross-links, and are expected to decrease the modulus and increase the swelling ratio relative to the ideal network. Loops in which the both cysteines on the same ERE chain react with two arms of the same PEG-4VS polymer generate an elastically ineffective chain that does not contribute to the modulus. Finally, entanglements formed during cross-linking are expected to act as virtual cross-links, increasing the modulus and decreasing the swelling ratio.

Next, the stoichiometry of the functional groups (r) was varied from 0.6:1 to 1.4:1 while maintaining the total polymer concentration in the gelation reaction at 15 wt% (Figure II-6). Altering the reactant stoichiometry potentially creates defects in the resulting network that are expected to affect the mechanical properties and swelling behavior of the hydrogels. When ERE is in stoichiometric excess (r = 0.6 or 0.8), ERE networks are more swollen, which suggests that the cross-linking density is lower. When PEG-4VS is added in excess (r = 1.2 or 1.4), there is not a significant difference in the mass swelling ratio compared to gels prepared with r = 1. A similar

Initial polymer concentration	$w_{ERE,sol}$	α	β	p	ν (mM)	μ (mM)
7.5 wt%	0.44%	0.43	0.27	0.79	1.1	0.7
10 wt%	0.42%	0.37	0.23	0.81	1.8	1.1
15 wt%	0.33%	0.29	0.17	0.85	4.9	2.8
20 wt%	0.26%	0.23	0.13	0.88	7.1	3.9
25 wt%	0.34%	0.24	0.13	0.88	8.8	4.9

Table II-3. Estimation of the concentration of elastically effective chains ν and cross-link denisty μ by Miller-Macosko Theory. The weight fraction of protein in the sol phase ($w_{ERE,sol}$) was measured by the BCA protein quantitation assay and used to determine β, the probability that a thiol functional group on ERE is not connected to the infinite network. β was used to calculate α, the probabilty that a vinyl sulfone group on PEG-4VS is not connected to the infinite network, and p, the extent of reaction. α and β were used to calculate ν and μ.

Initial polymer concentration	As-prepared modulus (kPa)			Swollen modulus (kPa)		
	G_{af}	G_{ph}	G'_e	G_{af}	G_{ph}	G'_e
7.5 wt%	2.8	1.1	1.0	2.0	0.7	1.0
10 wt%	4.5	1.8	2.1	3.2	1.3	1.8
15 wt%	12.2	5.3	5.3	8.3	3.6	3.4
20 wt%	17.6	7.9	8.9	11.6	5.2	7.3
25 wt%	21.8	9.8	14.2	13.9	6.2	10.8

Table II-4. Estimation of the modulus by the affine and phantom network approximations. The concentration of elastically effective chains ν and the cross-link density μ reported in Table II-3 and the swelling ratio were used to compute G_{af} and G_{ph} using Eq. II-1 and Eq. II-2, respectively.

effect was also observed for the storage moduli of the swollen gels. The modulus increased from r = 0.6 to 1, but was essentially unchanged from 1 to 1.4. When the vinyl sulfone is present in excess, it may potentially react with other nucleophiles such as the N-terminal amine to generate additional cross-links, minimizing the number of dangling chains. Alternatively, the low molecular weight dangling PEG chains (2.5 kDa per arm) may have a smaller effect on the stiffness and swelling behavior than dangling ERE chains (18.5 kDa). Additional experiments at larger values of r are required to determine if the gels eventually become softer and more swollen when the vinyl sulfone is present in greater excess.

The gelation conditions used to prepare the ERE hydrogels discussed above are not compatible with cell encapsulation due to the high concentration of guanindium chloride protein denaturant as well as the triethanolamine, which is potentially toxic to certain cell types [19]. An alternative cross-linking condition was investigated in which ERE and PEG-4VS were dissolved in HEPES buffered saline, pH 7.4 without triethanolamine. This buffering system was used previously to cross-link PEG-divinyl sulfone and peptides containing three cysteine residues with gelation times of several minutes [38]. Because softer, more swollen gels are expected to be better for 3D cell culture, ERE hydrogels were prepared at initial polymer concentrations of 5, 7.5 and 10 wt% and r = 1. The moduli of the gels in the as-prepared state and after swelling in PBS were similar to gels prepared under denaturing conditions (Figure II-7), confirming that the denaturant and organic base are not required for cross-linking ERE hydrogels.

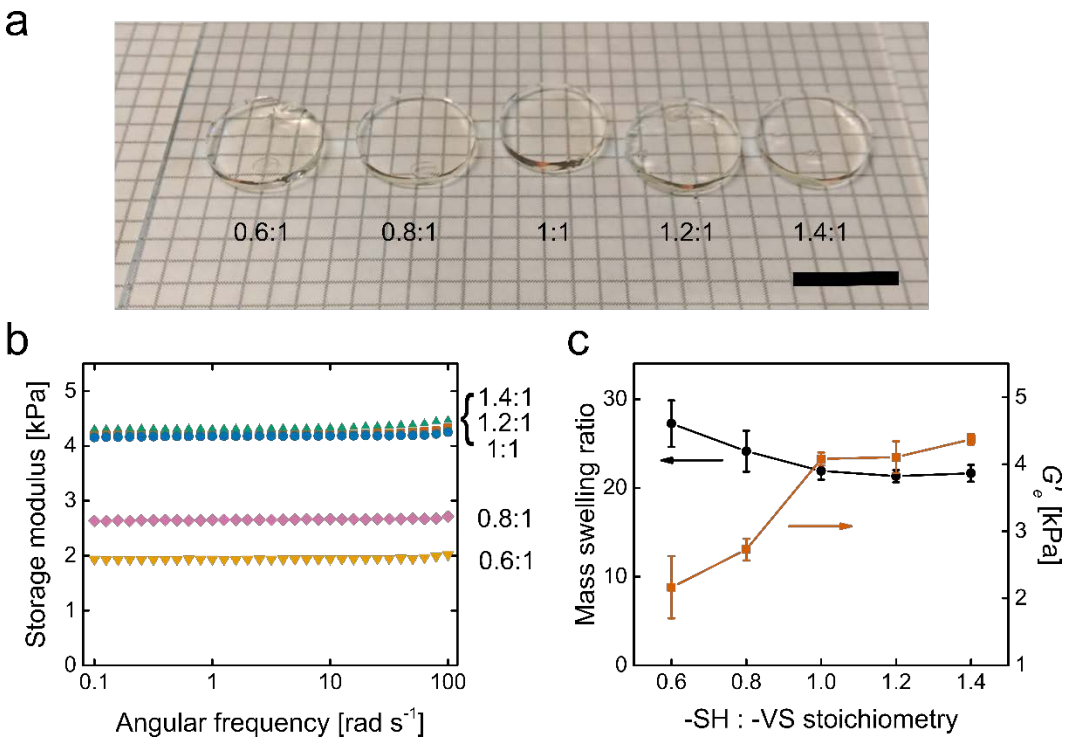

Figure II-6. Variation of the vinyl sulfone to thiol stoichiometry between 0.6-1.4. (**a**) Photographs of swollen ERE hydrogels. (**b**) Representative frequency sweep experiments show the storage moduli of ERE hydrogels prepared at different vinyl sulfone to thiol stoichiometry after swelling to equilibrium in PBS. (**c**) The mass swelling ratio decreases as r is increased from 0.6 to 1, but does not vary from r = 1 to 1.4 (n = 6 gels, avg. ± s.d.). Likewise, the equilibrium modulus G'_e increases as r is increased from 0.6 to 1, but does not vary from r = 1 to 1.4 (n = 3, avg. ± s.d.). The frequency sweep experiments in (b) were performed at 5% strain amplitude, 25 °C. The scale bar in (a) is 1 cm.

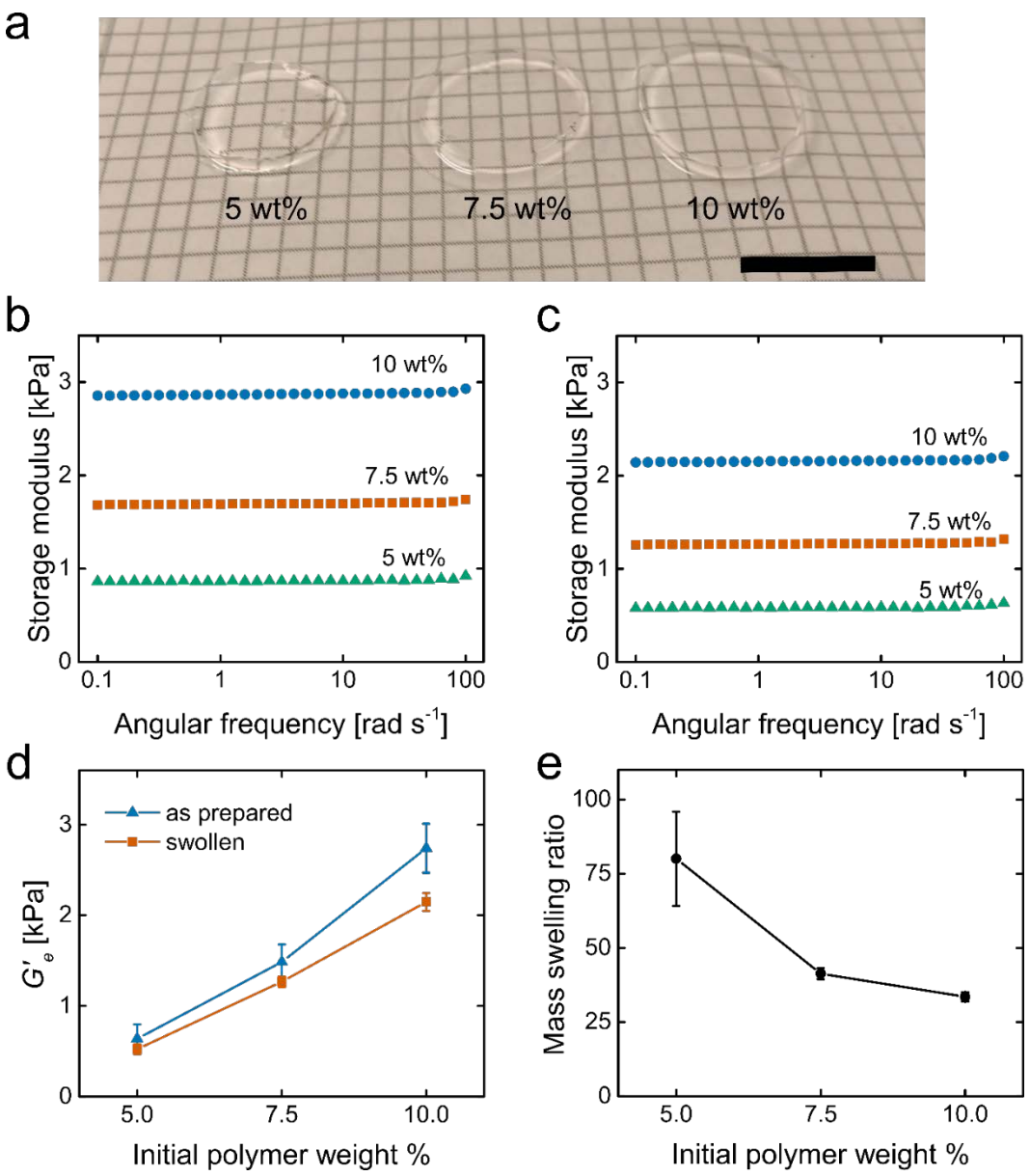

Figure II-7. Cross-linking ERE in HEPES buffered saline. (**a**) Photographs of swollen ERE hydrogels. (**b**) Representative frequency sweep experiments show the storage moduli of ERE hydrogels at initial polymer concentrations of 5, 7.5, and 10 wt% in the as-prepared state. (**c**) Representative frequency sweep experiments show the storage moduli of ERE hydrogels swollen to equilibrium in PBS. (**d**) The equilibrium modulus G'_e increases with increasing polymer concentration in the cross-linking reaction (n = 3, avg. ± s.d.). (**e**) The mass swelling ratio after swelling to equilibrium in PBS decreases as the initial polymer concentration is increased (n = 6 gels, avg. ± s.d.). All frequency sweep experiments were performed at 5% strain amplitude, 25 °C. Scale bar in (a) is 1 cm.

4.4 Gelation Kinetics

The gelation kinetics of 5, 7.5, and 10 wt% hydrogels with 1:1 functional group stoichiometry were determined by a dynamic oscillatory time sweep at 5% strain amplitude and 10 rad s^{-1} at 37 °C (Figure II-8 a). The gel point was determined from the time at which *G'* and *G"* intersect. At short times below the gel point, the mixture is a viscous solution and *G"* is larger than *G'*. After the gel point is reached, energy is stored in the forming network and *G'* is greater than *G"*. The storage modulus continues to increase rapidly before eventually approaching a plateau. The gelation time decreased as the amount of polymer was increased (Figure II-8 b). Gelation of 10 wt% mixtures occured within about 12 min. Gelation of 7.5 wt% and 5 wt% mixtures occur within 20 min and 43 min, respectively. This trend is expected assuming that covalent bond formation between ERE and PEG-4VS is a second order reaction with a rate that is proportional to the product of the reactant concentrations.

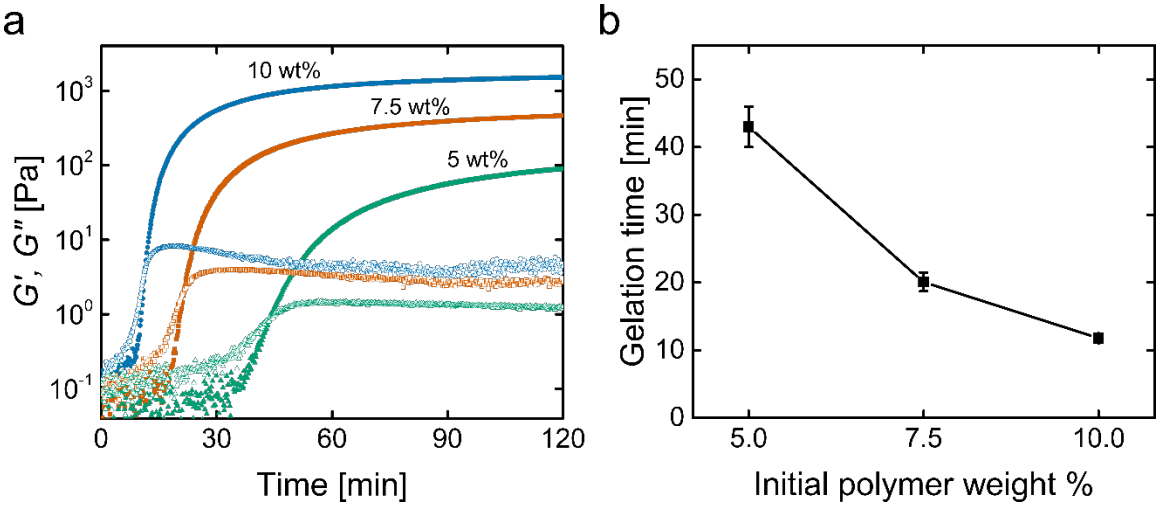

Figure II-8. Kinetics of ERE gelation. (**a**) Dynamic oscillatory time sweep of 5, 7.5, and 10 wt% ERE solutions cross-linked with PEG-4VS (*r* = 1:1) in HEPES buffered saline at 5% strain amplitude, 10 rad s^{-1}, 37 °C. The gel point is taken as the time at which *G'* (filled symbols) and *G"* (open symbols) intersect. (**b**) The gelation time decreases as the polymer concetration is increased (*n* = 3, avg. ± s.d.).

4.5 Preliminary Cell Encapsulation Experiments

The gelation conditions assessed in the previous sections were also evaluated in a cell encapsulation experiment with NIH 3T3 mouse fibroblasts. Cells were added to 5, 7.5, and 10 wt% ERE solutions in HEPES buffered saline at a concentration of 3×10^6 mL^{-1}, followed by cross-linking with PEG-4VS at r = 1:1. The hydrogel was formed as a droplet on a glass-bottom culture dish. After 1-2 hr at 37 °C (depending on the polymer concentration), complete growth medium was added. The gels were stained 3 days later with dyes that label either live or dead cells to evaluate cell viability and morphology. The gelation appeared to proceed normally in the presence of the fibroblasts, although the mechanical properties of the cell-laden hydrogels were not assessed.

Live cells were observed in all three ERE gels; however, they exhibited striking differences in their morphology in the different gel preparations (Figure II-9). In 5 wt% gels, most cells exhibited an elongated, spindle-like morphology. In 7.5 and 10 wt% gels, the cells were mostly round, although some cellular extensions could be observed, particularly in 7.5 wt% gels. The different cellular morphologies suggest that the fibroblasts spread more easily in a softer, more swollen matrix than in a stiffer, denser gel like those prepared at higher polymer concentrations. A similar trend has been reported for myoblast spreading in 4-arm PEG maleimide and 4-arm PEG vinyl sulfone hydrogels [19]. It is also noted that several cells are located in close proximity to one or more other cells, indicating that cells may not only survive in ERE gels but also proliferate.

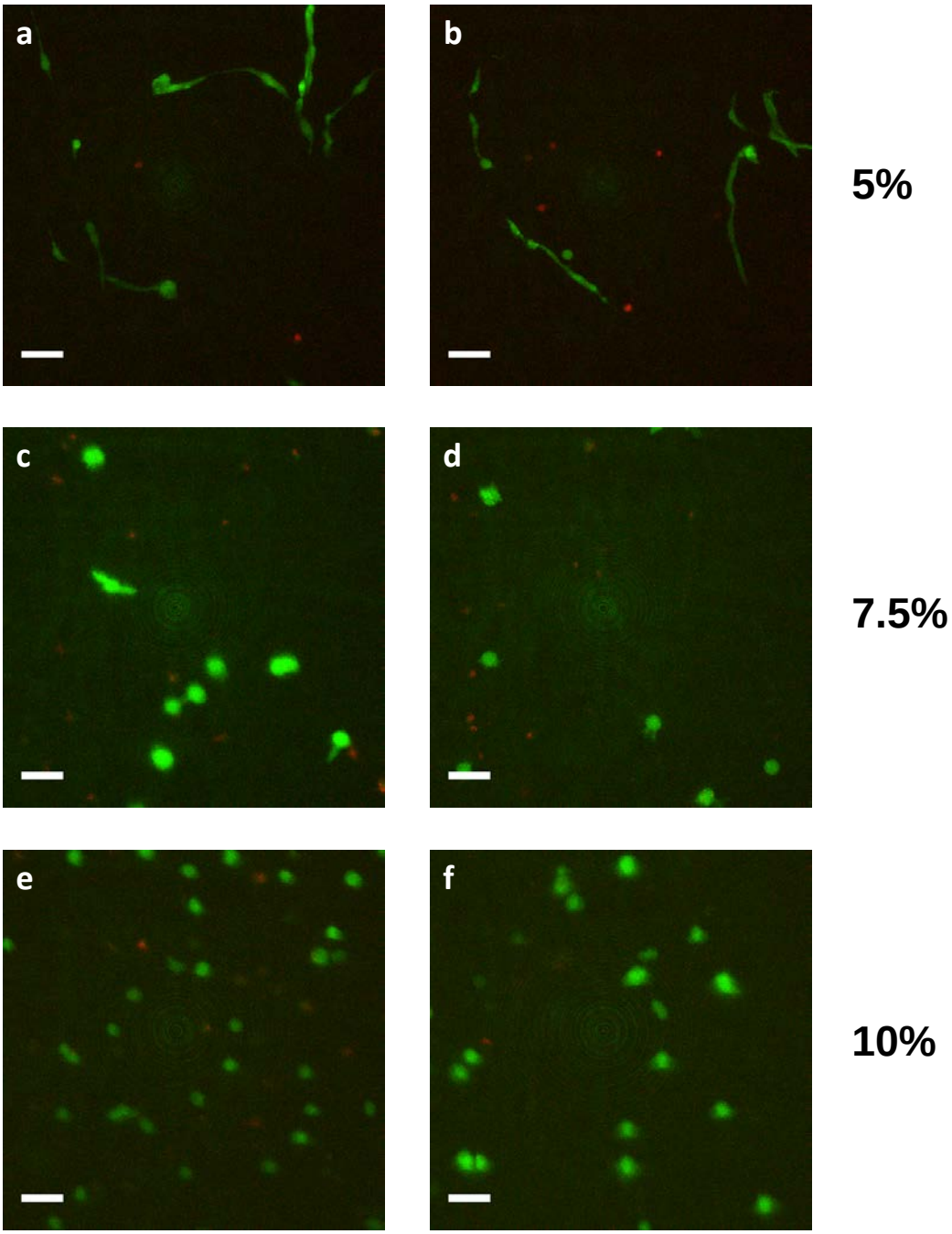

Figure II-9. Encapsulation of NIH 3T3 mouse fibroblasts in ERE gels. Projection of z-stacks acquired every 10 μm over a volume spanning a 200 μm thick section of gel. Live cells are stained with calcein AM (green). Dead cells are stained with ethidium homodimer-1 (red). The left and right panels are z-projections of two different x-y planes of the same gel. (**a**), (**b**) 5% ERE gel. (**c**), (**d**) 7.5 wt% ERE gel. (**e**), (**f**) 10 wt% ERE gel.

5. Conclusions

A new artificial protein ERE was designed and cross-linked into hydrogel networks. ERE was purified from a recombinant host with excellent yields using inverse temperature cycling with a free thiol content of approximately 90% of the expected value. End-linking ERE with PEG-4VS through a Michael-type addition reaction resulted in an optically clear hydrogel network. The mechanical properties of this network were engineered by systematic variation of the protein concentration during cross-linking and the stoichiometry of the protein and PEG cross-linker. In this way, the moduli of ERE networks were varied from 0.5 kPa to greater than 10 kPa. Biological activity was encoded directly within the ERE protein sequence in the form of a cell-binding domain and an MMP-cleavable peptide, potentially providing cues for directing the behavior of encapsulated cells. NIH 3T3 fibroblasts encapsulated in ERE hydrogels survived the cross-linking reaction and exhibited a spindle-like morphology in the softest material. This work demonstrates that end-linking artificial proteins is a promising strategy for engineering hydrogels with well-defined physical and biological properties.

6. Acknowledgements

Preliminary cross-linking and rheology experiments were conceived and performed with Dr. Wen-bin Zhang (W.-B.Z.) and Dr. Tomoyuki Koga. The ERE protein was designed by W.-B.Z. An early draft of a manuscript from which this chapter was adapted was written with W.-B.Z. The rheological experiments were performed in the laboratory of Professor Julia Kornfield. The protein mass spectrometry was performed at the Mass Spectrometry Facility in the Division of Chemistry and Chemical Engineering with assistance from Dr. Mona Shahgholi. The microscopy experiments were performed at the Biological Imaging Facility in the Beckman Institute.

7. References

[1] K.Y. Lee, D.J. Mooney *Chem. Rev.* **2001** *101*, 1869-1880.

[2] A. Panitch, T. Yamaoka, M.J. Fournier, T.L. Mason, and D.A. Tirrell *Macromolecules* **1999** *32*, 1701-1703.

[3] R.A. McMillan, V.P. Conticello *Macromolecules* **2000** *33*, 4809-4821.

[4] K. Di Zio, D.A. Tirrell *Macromolecules* **2003** *36*, 1553-1558.

[5] K. Trabbic-Carlson, L.A. Setton, A. Chilkoti *Biomacromolecules* **2003** *4*, 572-580.

[6] D.W. Lim, D.L. Nettles, L.A. Setton, A. Chilkoti *Biomacromolecules* **2007** *8*, 1463-1470.

[7] J.N. Renner, K.M. Cherry, R.S.C. Su, J.C. Liu *Biomacromolecules* **2012** *13*, 3678-3685.

[8] C. Chung, K.J. Lampe, S.C. Heilshorn *Biomacromolecules* **2012** *13*, 3912-3916.

[9] E.R. Welsh, D.A. Tirrell *Biomacromolecules* **2000** *1*, 23-30.

[10] P.J. Nowatzki, D.A. Tirrell *Biomaterials* **2004** *25*, 1261-1267.

[11] E. Fong, D.A. Tirrell *Adv. Mater.* **2010** *22*, 5271-5275.

[12] N.E. Davis, S. Ding, R.E. Forster, D.M. Pinkas, and A.E. Barron *Biomaterials* **2010** *31*, 7288-7297.

[13] M.K. McHale, L.A. Setton, A. Chilkoti *Tissue Eng.* **2005** *11*, 1768-79.

[14] C.A. DeForest, B.D. Polizzotti, K.S. Anseth *Nat. Mater.* **2009** *8*, 659-664.

[15] A.M. Testera, A. Girotti, I.G. Torre, L. Quintanilla, M. Santos, M. Alonso, and J.C. Rodríguez-Cabello *J. Mater. Sci. Mater. Med.* **2015** *26*, 1-13.

[16] F. Sun, W.-B. Zhang, A. Mahdavi, F.H. Arnold, and D.A. Tirrell *Proc. Natl. Acad. Sci. USA* **2014** *111*, 11269-11274.

[17] S.D. Tilley, N.S. Joshi, M.B. Francis, in *Wiley Encyclopedia of Chemical Biology*, Vol. 4 Wiley, New York **2007**.

[18] M.P. Lutolf, J.A. Hubbell *Biomacromolecules* **2003** *4*, 713-722.

[19] E.A. Phelps, N.O. Enemchukwu, V.F. Fiore, J.C. Sy, N. Murthy, T.A. Sulchek, T.H. Barker, and A.J. García *Adv. Mater.* **2012** *24*, 64-70.

[20] S.C. Rizzi, J.A. Hubbell *Biomacromolecules* **2005** *6*, 1226-1238.

[21] C.L. McGann, R.E. Akins, K.L. Kiick *Biomacromolecules* **2016** *17*, 128-140.

[22] D. Xu, D. Asai, A. Chilkoti, S.L. Craig *Biomacromolecules* **2012** *13*, 2315-2321.

[23] D.T. McPherson, J. Xu, D.W. Urry *Protein Expression Purif.* **1996** *7*, 51-57.

[24] P. Eyer, F. Worek, D. Kiderlen, G. Sinko, A. Stuglin, V. Simeon-Rudolf, and E. Reiner *Anal. Biochem.* **2003** *312*, 224-227.

[25] T.K.L. Meyvis, S.C. De Smedt, J. Demeester, W.E. Hennink *J. Rheol.* **1999** *43*, 933-950.

[26] M.D. Pierschbacher, E. Ruoslahti *Nature* **1984** *309*, 30-33.

[27] A.L. Main, T.S. Harvey, M. Baron, J. Boyd, and I.D. Campbell *Cell* **1992** *71*, 671-678.

[28] U. Hersel, C. Dahmen, H. Kessler *Biomaterials* **2003** *24*, 4385-4415.

[29] H. Nagase, G.B. Fields *Peptide Science* **1996** *40*, 399-416.

[30] M.P. Lutolf, J.L. Lauer-Fields, H.G. Schmoekel, A.T. Metters, F.E. Weber, G.B. Fields, and J.A. Hubbell *Proc. Natl. Acad. Sci. USA* **2003** *100*, 5413-5418.

[31] H. Wang, L. Cai, A. Paul, A. Enejder, and S.C. Heilshorn *Biomacromolecules* **2014** *15*, 3421-3428.

[32] D.W. Urry *J. Phys. Chem. B* **1997** *101*, 11007-11028.

[33] G.L. Ellman *Arch. Biochem. Biophys.* **1959** *82*, 70-77.

[34] D.R. Miller, C.W. Macosko *Macromolecules* **1976** *9*, 206-211.

[35] M. Rubinstein, R.H. Colby, *Polymer Physics* Oxford University Press, Oxford **2003**.

[36] M.A. Lillie, J.M. Gosline *Biopolymers* **2002** *64*, 115-126.

[37] 2012. *Polyethylene glycol [MAK Value Documentation, 1998]*. *The MAK-Collection for Occupational Health and Safety*. 274-270.

[38] A.B. Pratt, F.E. Weber, H.G. Schmoekel, R. Müller, and J.A. Hubbell *Biotechnol. Bioeng.* **2004** *86*, 27-36.